Effect of preliminary treatment on the superficial morphology and the corrosion behaviour of AA2024 aluminum alloy

E. A. Matter[a],*, S. V. Kozhukharov[b], M. S. Machkova[b]

a) Chemistry Department, Faculty of Science, Damanhour University, 22111 Damanhour, Egypt.
b) University of Chemical Technology and Metallurgy, 8 Kl. Ohridski St, 1756 Sofia, Bulgaria.

The effect of the superficial preliminary treatment on the properties of the oxide film and its influence on the corrosion behaviour of AA 2024 aluminum alloy in 3.5% NaCl solution was investigated. It was done applying crystallographic optical and atomic force microscopic techniques, combined with electrochemical measurements - linear voltammetry (LVA) and Electrochemical Impedance Spectroscopy (EIS).

Three approaches were used for preliminary treatments of the samples, as follows: only degreasing (without removal of oxide film), mechanical polishing and a combination between mechanical polishing with etching in alkaline solutions. The parameters of the corrosion process (polarization resistance, pitting nucleation potential, impedance module and capacitance) were used as a quantitative measure for the effect of the preliminary treatment approach. It was established that the most effective pretreatment in terms of removal of the oxide layer is the mechanical polishing. The undertaken electrochemical measurements evidenced that the approach of etching in alkaline solutions, used in a large number of articles, causes a formation of a film, which could not be removed completely by desmutting with diluted solutions of HNO_3. Etching procedure could be appropriate for other Al-alloys but it is not recommended for the AA2024 alloy.

Keywords: preliminary treatment, corrosion, aluminum alloy - AA2024, EIS.

INTRODUCTION

The aluminum is a metal which possesses a distinguishable corrosion resistivity in a water media. It is well known that the reason for this is the formation of a natural oxide layer, which is usually present on its surface. In neutral environments, this film consists generally of boehmite γ-AlO(OH) mineral [1]. According to ref. [1] it has relatively low thickness (5nm), as well as low electronic conductivity, which strongly hinders the oxidation and the reduction reactions in the corrosion process. In the case of Al-alloys, due to the extended mechanical strength and the relatively lower weight, they are accompanied coincidently by enhanced susceptibility to local corrosion impact. These alloys possess lower corrosion resistivity, due to the presence of intermetallics in the basic Al-matrix. These inclusions are in the form of particles, which become centers of nucleation and further spreading of local corrosion process. AA2024 alloy reveals peculiar aptitude to that kind of corrosion [2-5]. This alloy is generally used in the aircraft industry, but its application is possible only upon appropriate and effective anticorrosion protection [6].

In any case related to the protection methods, either by inhibitors or by protective coatings, the corresponding alloy samples undergo preliminary treatments in order to remove the superficial oxide layer. There is a large variety of methods which are based on two general approaches: a) mechanical treatment [7-9] by grinding with emery paper and b) chemical by dissolution of the film in alkaline solutions [10-12]. No description for the reasons of approach selection is found in the literature. Logically, a comparison between the above approaches and their impact over the AA2024 behavior in a corrosive medium is necessary.

It seems that one of the reasons for the contradictive results, described by different authors [3-12], as well as the unsatisfactory reproduction of such results, could be ascribed to the difference in the approaches, applied for the preliminary treatments.

The aim of the present work is to study the effect of the preliminary treatment on the superficial morphology of the AA2024 alloy which predetermines its behavior in corrosive media. In addition, a detailed description of the preliminary treatment effect on the parameters of the corrosion process and their evolution within the exposure time, for the AA2024 aluminum alloy in an aggressive Cl^- ions media was done.

* To whom all correspondence should be sent:
E-mail: e_a_matter@yahoo.com

EXPERIMENTAL

2.1. AA2024 aluminum alloy composition

The composition is presented in Table 1, determined by Induction Coupled Plasma (ICP–OES) analysis upon decomposition in a mixture of acids.

Table 1. Composition of AA2024 aluminum determined by ICP – OES analysis.

Element	Concentration (wt. %)
Al	remainder
Cu	3.716
Fe	0.404
Mg	1.259
Mn	0.537
Ni	0.055
Si	<0.01

2.2. Preliminary treatment of the samples

AA2024 metal plates with thickness of 2 mm underwent the following preliminary treatment procedures:

S_1- As received, only degreasing in Ethanol/Ether 1:1 (10 min) and final washing vigorously with distilled water. It should be noticed that the natural oxide layer is not removed in this case;

S_2- Polished, using emery paper, in the following order: 240-360-500-800 grits. Then degreased by Ethanol/Ether 1:1 (10 min) and finally washed with distilled water;

S_3- Polished, using emery paper as described above, degreased with Ethanol/Ether 1:1 (10 min), washed with distilled water, after that chemically treated with a mixture of [NaOH (40gm/l) + Na_3PO_4 (30gm/l) + Na_2CO_3 (20gm/l) for 3 min at 60 ^{o}C], then desmutted by [$HNO_3 : H_2O$ (1:1)] solution for 2 min, at room temperature, and finally washed by distilled water.

The corresponding methods of preliminary treatment procedures either could be found in various articles [3-12] or recommended in handbooks [13, 14].

2.3. Superficial morphology measurements

a. Optical metallographic microscopy

It was carried out using BOECO metallographic microscope. The image measurements were obtained by web-camera with 600 x 800 pixel resolution at a magnification of 40X.

b. Atomic Force Microscopy

The observations were performed by EasyScan 2 AFM, supplied by Nanosurf,

Switzerland, supported by TAP190G cantilever, produced by Budgetsensors, Bulgaria. The measurements were done at a square area of 49.5 µm linear size. The resolution was 256 points/line, at an imaging rate of 2 seconds per line. The images were obtained in a "scan forward" mode and the scan mode was from down to up, performed in static regime.

2.4. Electrochemical measurements

For the purpose, three-electrode electrochemical cell with a volume of 100 ml was used. The area of each sample, serving as a working electrode, was about 2.0 cm^2. A platinum net in a cylindrical form was used as counter electrode. Its surface area was relatively two orders of magnitude higher than that of the working electrode, in order to avoid the influence of its superficial capacitance on the experimental results [15, 16]. All potential values of the working electrode were measured using Ag/AgCl standard reference electrode, model 0726100, produced by Metrohm, with a potential of $E(Ag^+/ AgCl) = 0.2224V$ (with 3M KCl).

AUTOLAB PGStat 30/2 potentiostat-galvanostat, produced by ECO CHEMIE B.V. in the Netherlands, with additional FRA-2 frequency response analyzer, was used for the both kinds of electrochemical measurements. Each linear voltammetric measurement was carried out after acquiring of the respective impedance spectrum in order to eliminate any possible changes of the electrode surface due to the high polarization. The measurements were performed in the following sequence: initially cathodic polarization curves were recorded in the potential range from OCP + 0.03 V to OCP – 0.40 V with a potential sweep rate of 0.001 V/s. After recuperation of the OCP, the anodic polarization curves were recorded in the range from OCP - 0.03 V to OCP + 0.50 V. At least 3 samples underwent the same test procedures in order to obtain reliable results. The results of the most representative sample of each group were selected for the needs of this research work.

All the EISs were done at an OCP in the frequency range between 10^5 and 10^{-2} Hz at 7 frequencies per decade, and signal amplitude of 20 mV from peak to peak. The entire electrochemical cell was enclosed in Faraday cage, in order to avoid any outside electromagnetic influences. The corrosive medium was a 3.5 % NaCl solution with a pH= 6.60, served as a naturally aerated model corrosive medium (electrolyte). All measurements were carried out at a room temperature.

RESULTS AND DISCUSSION

3.1. Surface morphology

Figure 1 shows the optical metallographic images of the sample surface upon different pre-treatments prior to their immersion and after 24-hours of exposure into the corrosive solution. On Figure 2 are depicted the initial surface topographies obtained via AFM microscopy.
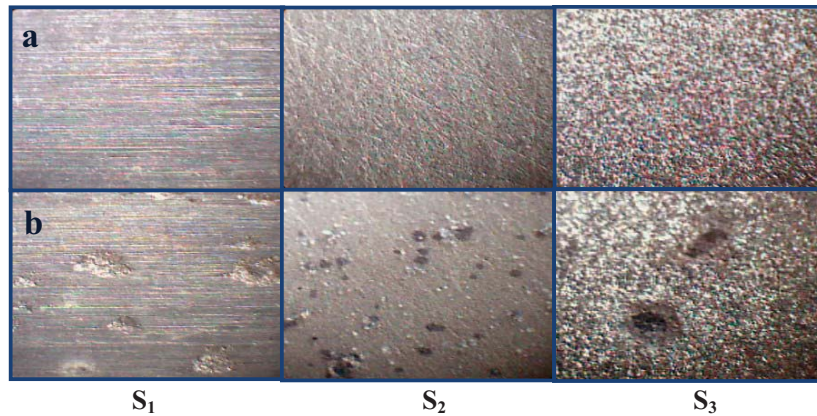

Fig. 1. Images obtained by Optical Metallographic Microscopy for samples S$_1$, S$_2$ and S$_3$ after superficial pretreatment (a) - before and (b) - after 24 hours exposure into the aggressive medium and subsequent anodic polarization.
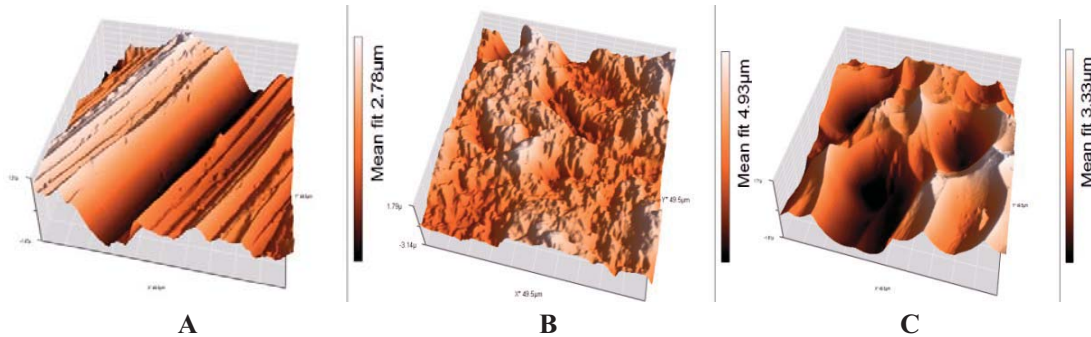

Fig. 2. Topographic images of the output surface obtained with AFM microscopy for A- degreased, B-mechanically polished and C-mechanical then etched with alkaline solutions samples.

One of the most interesting effects is seen in the surface morphology of the specimen after anodic polarization (Fig. 1-b). From the Figure is clear that a few corrosive spots are observed on sample surface which was only degreased (S$_1$ -procedure). The morphology of these spots is consequence of the thicker oxide layer on this sample, which predetermines the kinetics of the pitting growth. The pitting appears on the sites of defects in the layer only. Similar behaviour was established for the S$_3$ treatment procedure, as well. The products, of the surface etching remain in the form of insoluble layer and cannot be removed by desmutting in HNO$_3$/H$_2$O (1:1) solution.

In the case of mechanical pretreatment (S$_2$-procedure), the thick oxide layer, which is formed during the metallurgical production process, was removed. It was established that only very thin oxide film was formed during the exposure into the corrosive medium. The formed oxide layer was of uneven thickness and thinner in the areas where the intermetallic particles of the alloy elements (Al, Mg, Cu) exist, as mentioned by other authors [2-6]. According to Yasakau and co-workers [5], the most predominant among the various intermetallics is the S-phase (Al$_2$CuMg). The latter occupies more than 60% of all inclusions into the AA2024 alloy. Consequently, S-phase has the most significant contribution to the AA2024 behaviour. Namely, the S-phase superficial areas, possess defects in the oxide film. The chloride anions in the solution predominantly attack these areas and form pitting centers which due to their large number grow slowly and do not stimulate development of crevice corrosion.

3.2. Electrochemical measurements

a. Polarization measurements

Figure 3 shows that the variation of OCP with the exposure time is remarkably different depending on the technique, applied in the preliminary

treatment. OCP of the S_1 sample oscillates around a defined value, remaining almost unchanged even after 24 hours. Similar behaviour is observed also in the case of the sample, etched by the S_3 procedure. Similar oscillations of OCP are also described by Schem and co-authors [10]. According to them, these oscillations are indicative for permanent nucleation and repassivation of pitting.

The observed differences of the shapes of OCP-time curves of all samples could be explained by the Yasakau concepts [5]. Intermetallics are formed in the AA2024 structure as particles with different size and composition. The most widespread among them is named "S-phase" with Al_2CuMg composition. Al is presented consequently in both, the basic matrix and the intermetallics. The corrosion mechanism of the AA2024 alloy is described in details by Yasakau and co-workers [5].
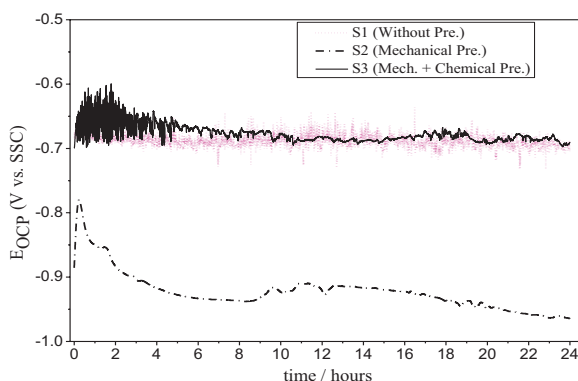

Fig. 3. Open Circuit Potential - time curves of samples prepared with different approaches of preliminary treatment during the exposure to 3.5 % NaCl.

When the polished sample (S_2) is exposed into the model corrosive medium, *chemical selective dissolution* of Al and Mg from the S-phase begins, causing enrichment of the surface by copper remnants. The latter, shift the OCP to more positive values (Fig. 3, curve S_2). The copper enriched remnants become cathodic areas, relative to the aluminum matrix, which in that case reveals anodic behaviour. As a consequence, galvanic couples appear, promoting *electrochemical dissolution* of Al from the anodic zones. After that moment, accelerated rate of the anodic reaction causes shift of the OCP values towards the negative direction. Moreover, the evolution of the OCP values in the case of S_3 and S_1 is similar due to the fact that the surfaces of both are covered by oxide film.

Figure 4 shows the cathodic and anodic potentiodynamic polarization curves of the samples upon different superficial treatments and different duration of exposition to corrosive medium (3.5 % NaCl). It could be seen that the sample with a

natural oxide layer (S_1), compared to the rest of the samples, shows the lowest cathodic currents (Fig. 4-a). Evidently is that the cathodic partial reaction is more remarkably hindered by both, the higher thickness and the lower electronic conductivity. This film is removed afterwards, either by mechanical polishing (S_2) or by etching in alkaline solutions (S_3). Cathode currents increase with one order of magnitude, achieving almost the same values.
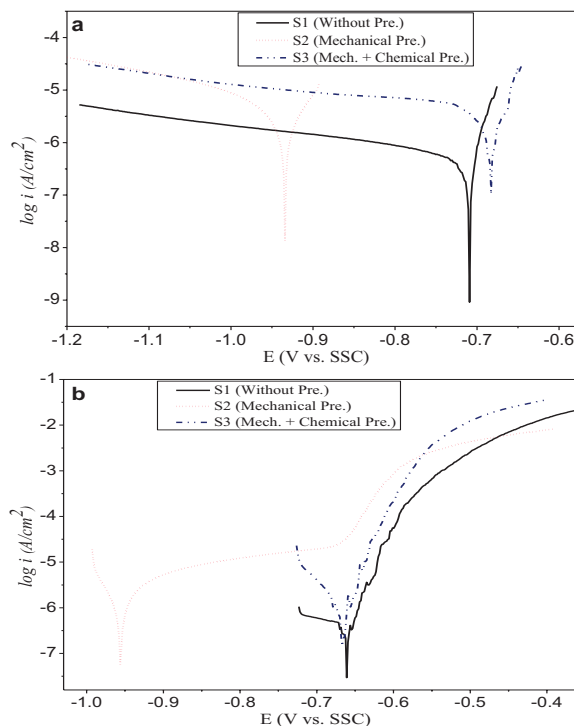

Fig. 4. Potentiodynamic cathodic- (a) and anodic- (b) polarization curves of samples prepared with different approaches of preliminary treatment after 4h exposure to 3.5% NaCl solution.

It seems that the superficial sediments, formed during etching, possess relatively high electronic conductivity because it does not suppress the cathode partial reaction of oxygen reduction. The anodic partial polarization curves of S_1 and S_3 treatments (Fig. 4-b) after 4 hours of exposure are almost identical and they have not got any passive region. The absence of such region means that there is overlapping between the corrosion potential and the potential of pitting nucleation [17].

The shape of the anodic polarization curve of the mechanically treated sample (S_2) is quite different. The corrosion potential of this sample is shifted into a negative direction as a result of acceleration of the anodic polarization reaction. The corrosion products, formed on the surface of the

samples, cause the appearance of anodic current plateau. At higher polarization, when the pitting formation potential is reached, a sharp rise of the current density begins and becomes almost equal to the current values of the S_1 and S_3 samples.

b. EIS measurements

The application of this method gives a possibility to clarify the nature of the physical and chemical processes in the bulk of the individual phases and their boundaries in the entire metal/electrolyte system. Figure 5 shows the impedance spectra in Bode and Nyquist plots for the samples after 2 hours of exposure to a corrosive medium. Clearly defined maximum at the average frequency range (from 10^2 to 0.5 Hz) is observed in the spectra of all samples. This maximum is related to the time-constant τ = RC, originated from the parallel connection between the resistance R and the capacitance C.
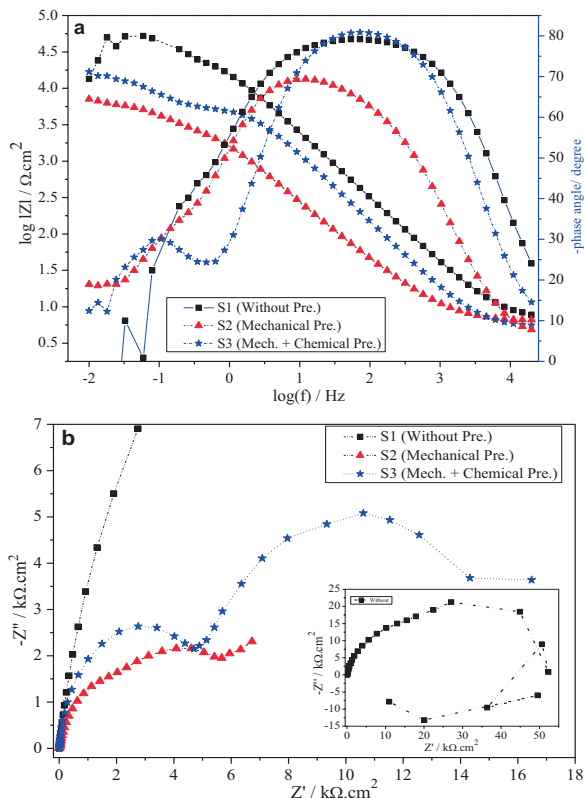
increases after a prolonged time of exposure. This phenomenon is particularly expressed after a 24-hour exposure (Fig. 6).

The evolution of the dependence of the phase shift- φ versus the frequency- f, suggests that during the exposure to the corrosive medium, the electrolyte penetrates the oxide film and as a consequence two noticeable oxide layers appear. Both layers are represented in the impedance spectrum by one joined double time-constant. Both layers could be ascribed to the natural oxide film and to the additionally formed oxide film due to the hot-rolling process during production of the said Al-sheets.

The impedance behaviour is rather different at the lowest frequencies. Pseudo inductance appears when the thick oxide layer is not removed in the case of S_1. It is expressed in positive values of both, the imaginary component of the impedance Z and the phase shift φ. This behaviour, according to ref.

Fig. 5. Bode (a) and Nyquist (b) plots of samples after different approaches of preliminary treatment and after 2h exposure into 3.5% NaCl solution.

In this particular case R and C correspond to resistance and capacitance of the superficial oxide layer, R_{oxy}, and its capacitance, C_{oxy}. Thus, the development of this time constant for the degreased S_1 sample is extremely interesting. The comparison of spectra of S_1 with different exposure times reveals that the medium frequency maximum range
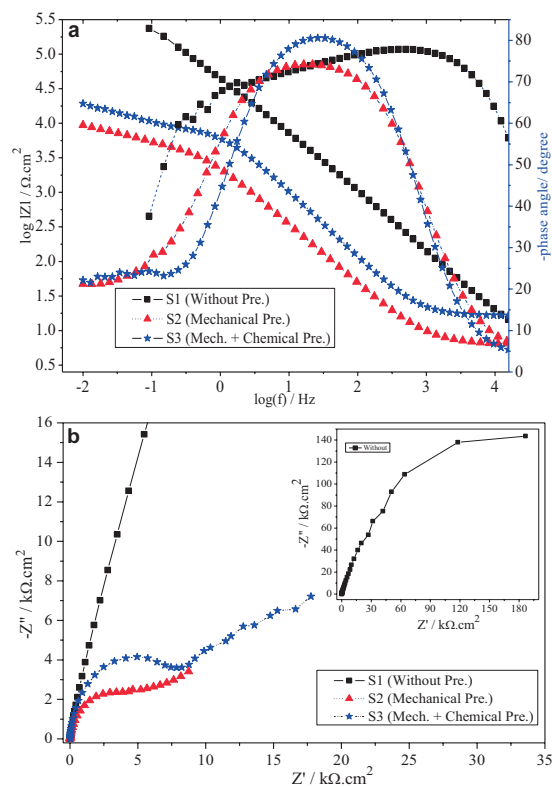
Fig. 6. Bode -(a) and Nyquist -(b) plots of samples after different approaches of preliminary treatment and after 24h exposure to 3.5% NaCl solution.

[18], owes its origin to pitting nucleation in the oxide layer. Other authors [19] suggest that this behaviour is a consequence of particle involvement in the oxide layer. The inductance completely disappears after achievement of a stationary state (Fig. 6-a).

The samples, treated using different approaches, reveal different values of the total impedance (impedance modulus) at a frequency of 10^{-2} Hz. Usually, these values are related to the protective properties of the oxide film. Figures 5 and 6 undoubtedly demonstrate that the impedance module (Z) value for S_1 is in orders of magnitude higher than those of the remaining samples. It is due to the formation of two oxide layers. On the other hand, the impedance module Z for S_2 possesses the lowest value because of the complete removal of the superficial oxide layer, which is actually the main aim of each pretreatment. In addition, the values of the impedance modulus are relatively higher for the etched S_3 sample, compared to the mechanically treated S_2 sample. This fact confirms the observation that the etching in alkaline media leads to formation of an insoluble film, thus increasing the total resistance at an alternate current.

Structural Impedance Modeling was carried out in order to obtain numeric values for the corrosion parameters of the samples presented in Table 2. This procedure allows the electrochemical system to give all resistive (R) and capacitive (C) response by fitting it to the appropriate equivalent circuit.

For the purposes of the present study an appropriate equivalent circuit was chosen. According to Boukamp [20], it could be described as follows: $R_{el}(Q_{oxy}[R_{oxy}(Q_{dl} R_p)])$, where R_{el}, R_{oxy}, and R_p are the resistances of the electrolyte, the oxide layer, and the charge transfer at the interface metal-oxide (also known as a polarization resistance). Q_{oxy} and Q_{dl} are the Constant Phase Elements (CPE) used to approximate the values of the respective capacitances of the oxide layer and the double electric layer. The mentioned approximation is always used when the phase shift of the electric current sinusoid is less than 90º with respect to the potential. The impedance of the constant phase element depends on the frequency, like the capacitance. Therefore, it could be presented by the following equation:

$$Q = Y_0^{-1}(j\omega)^{-n}$$

where Y_0 and n are frequency independent constants, ω – angular frequency and j- imaginary unite. Once the constant- n has values in the range of 0.8 to 1, the respective CPE could be accepted as capacitance. Straight tails appear at the lowest frequency range in the Nyquist plots for some of the samples revealing the presence of diffusion process.

Table 2. Corrosion parameters for S_1, S_2 and S_3 samples vs. time treatment.

PARAMETERS	The equivalent circuit: $R_{el}(Q_{oxy}[R_{oxy}(Q_{dl} R_p)])$								
	S_1			S_2			S_3		
	2 h	4 h	24 h	2 h	4 h	24 h	2 h	4 h	24 h
R_L ($\Omega.cm^2$)	6.67 ± 0.077	5.24 ± 0.10	5.71 ± 0.18	6.35 ± 0.1	11.7 ± 0.04	6.32 ± 0.037	5.31 ± 0.067	5.4 ± 0.089	16.5 ± 0.08
R_{oxy} ($k\Omega.cm^2$)	33.7 ± 1.23	35 ±1.87	22.01 ± 3.97	4.38 ± 0.42	3.5 ± 0.05	5.22 ± 0.14	5.68 ± 0.09	3.5 ± 0.06	8.33 ± 0.13
Q_{oxy} Y_0, $S^n \Omega^{-1} cm^{-2}$	9.8E-6 ± 1.1E-7	1.6E-5 ± 2.5E-7	3.1E-6 ± 8.1E-8	1.2E-4 ± 3.5E-6	1E-4 ± 8.2E-7	7.7E-5 ± 8.0E-7	1.6E-5 ± 2.8E-7	1.7E-5 ± 4.5E-7	1.9E-5 ± 2E-7
n	0.89 ± 0.01	0.84 ± 0.002	0.89 ± 0.003	0.8 ± 0.004	0.83 ± 0.001	0.87 ± 0.002	0.93 ± 0.002	0.95 ± 0.004	0.95 ± 0.002
R_p ($k\Omega.cm^2$)	30.46 ± 9.08	13.96 ±2.67	391 ± 22.44	5.62 ± 2.04	1.1 ± 0.12	10.93 ± 1.66	11.04 ± 0.42	10.06 ±0.63	21.92 ± 1.59
Q_{dl} Y_0, $S^n \Omega^{-1} cm^{-2}$	4.1E-5 ± 2.9E-6	7.6E-5 ± 2.1E-5	2.0E-6 ± 1.1E-7	8.7E-4 ± 3.3E-4	0.001 ± 1.8E-4	7.7E-4 ± 7.4E-5	3.1E-4 ± 1.2E-5	5.6E-4 ± 2.5E-5	3.3E-4 ± 1.5E-5
n	1 ± 0.11	1 ± 0.13	0.73 ± 0.024	0.621 ± 0.15	1 ± 0.06	0.638 ± 0.04	0.915 ± 0.02	0.947 ± 0.03	0.683 ± 0.02
ω, $S^{0.5} \Omega^{-1}$	-	-	-	-	0.003± 2.1E-4	-	-	-	-

For these cases, supplementary Warburg element was added to the equivalent circuit. Table 2 presents values of the corrosion parameters, obtained by spectra fitting procedure to the equivalent circuits.

CONCLUSIONS

The influence of the AA 2024 aluminum alloy specimen superficial preliminary treatment over its morphology and corrosion behaviour in a 3.5% NaCl solution was studied. Three different approaches for a preliminary treatment of AA2024 metal plates were applied: S_1 – just degreased, S_2 – mechanically polished, and S_3 – mechanically treated and etched in alkaline solution. The investigation is done by applying crystallographic optical and atomic force microscopic techniques, combined with electrochemical measurements executed by linear voltammetry and Electrochemical Impedance Spectroscopy.

The analysis of the impedance spectra of the not treated samples (only degreased), reveals that they are covered by oxide film, consisting of two layers, a natural oxide layer, and a layer of additionally formed oxide during the metallurgical production process of the alloy. These samples show the highest impedance modulus, the highest polarization resistance, and respectively the lowest corrosion rate. It is established that they are not protected from the pitting corrosion process. The oxide layer possesses low number of defects and consequently, low number of pittings is formed during the exposure of the samples to the corrosion medium. These pittings are converted to crevice corrosion sites with a remarkable size. The reason for this phenomenon is that the pitting growth rate exceeds their nucleation rate.

The etching procedure in the alkaline solutions causes sediment coverage of alloy element oxides. These sediments can not be removed by desmutting with a diluted solution of HNO_3. The presence of these sediments is confirmed by the OCP behaviour within the exposure time in the corrosive medium.

It is established that the mechanically polished samples are always covered with a natural oxide layer after exposure in the corrosive medium. This film has the highest number of defects combined by the lowest values of impedance modulus, polarization and capacitive resistances. By this approach of preliminary treatment the oxide layer is almost completely removed**,** which is the purpose of the superficial treatment.

The following general conclusion with a significant importance for the practice could be made: the etching in alkaline solutions, used in a large number of articles referring various aspects of the corrosion of AA2024 alloy, is not recommended. However, it could be appropriate for alloys with other compositions. In the particular case of the AA2024 alloy, mechanical polishing could be recommended because the sample surfaces achieved a state close to the complete absence of an oxide layer.

REFERENCES

1. H. Kaesh, Die Korrosion der metalle, Springer-Verlag, Berlin, 1979.
2. M. Iannuzzi, G. S. Frankel, *Corr. Sci.* **49**, 2371 (2007).
3. J. R. Davis, ASM Specialty Handbook: Aluminum and Aluminum Alloys, ASM International, Chapter 2, 1993, pp.31–35.
4. C. Kammer, Aluminum Handbook first ed. Vol. Aluminum - Verlag 1999 (Chapter 4) pp. 125-143.
5. K. A.Yasakau, M. L. Zheludkevich, S. V. Lamaka, M. G. Ferreira, *J. Phys. Chem. B*, **110**, 5515 (2006).
6. G. S. Tsaneva, V. S. Kozhukharov, S. V. Kozhukharov, M. E. Ivanova, J. Gervann, M. Schem, T. Schimdt, *J. Univ. Chem. Techn. Met.* **43**, 231 (2008).
7. F. M. Queiroz, M. Magnani, I. Costa, H. G. De Melo, *Corr. Sci.* **50,** 2646 (2008).
8. M. Bethencourt, F.J. Botana, M. J. Cano, M. Marcos, J. M. Sanchez-Amaya, L. Gonzalez-Rovira, *Corr. Sci.* **51,** 518 (2009).
9. S. M. Tamborin, A. P. Maisonnave, D. S. Azambuja, G. E. Englerd, *Surf. Coat. Techn.* **202**, 2304 (2008).
10. M. Schem, T. Schmidt, J. Gerwann, M. Wittmar, M. Veith, G. E. Thompson, Ls. Molchan, T. Hashimoto, P. Skeldon, A. R. Phani, S. Santucci and M. L. Zheludkevich, *Corr. Sci.* **51**, 2304 (2009).
11. O. Lunder, J. C. Walmsley, P. Mack, K. Nisancioglu, *Corr. Sci.* **47,** 1604 (2005).
12. S. V. Kozhukharov, G. S. Tsaneva, V. S. Kozhukharov, J. Gerwann, M. Schem, T. Schmidt, M. Veith, *J. Univ. Chem. Techn. Met.* **43,** 73 (2008).
13. B. Pentchev, S. Detchev, Manual of Galvano-techniques, Technika, Sofia 1982.
14. L.Y. Kadaner , Manual of Galvanostegy, Technika Gov. Ed., Kiev, 1976.
15. B. B. Damaskin, O. A. Petrii, Fundamentals of theoretical Electrochemistry, Superior School, Moscow, 1978.

16. B. B. Damaskin, O. A. Petrii, Introduction to electrochemical kinetics, Superior School, Moscow, 1975.

17. M. Bethencourt, F. J. Botana, J. J. Calvino, M. Marco, M. A. Rodriguez-Cachon, *Corr. Sci.* **40**,1803 (1998).

18. Li Song-mei, Zhang Hong-rui, Liu Jian-hua, *Trans. Nonferrous Met. SOC. China* **17**, 318 (2007).

19. S. A. Rehim, H. H. Hassan, M. A. Amin, *Appl. Surf. Sci.* **187,** 279 (2002).

20. B. A. Boukamp, *Solid State Ionics*, **20**, 31 (1986).

ЕФЕКТ НА ПРЕДВАРИТЕЛНАТА ПОДГОТОВКА ВЪРХУ ПОВЪРХНОСТНАТА МОРФОЛОГИЯ И КОРОЗИОННОТО ПОВЕДЕНИЕ НА АЛУМИНИЕВА СПЛАВ АА 2024

Е.А. Матер[a],*, С.В. Кожухаров[b], М.С. Мачкова[b]

a) Департамент по химия, Научен факултет, Университет в Даманхур, 22111 Даманхур, Египет
b) Химико-технологичен и металургичен университет, бул.Кл. Охридски, 8, 1756 София

(Резюме)

Изследван е ефектът на повърхностната предварителна подготовка върху свойствата на оксидния филм и нейното влияние върху корозионното поведение на алуминиева сплав АА 2024 в 3.5% NaCl разтвор. Изследването е проведено, чрез оптична и атомно – силова микроскопски техники, съчетани с електрохимични изследвания - линейна волтамперометрия (ЛВА) и електрохимична импедансна спектроскопия (ЕИС).

За предварителна обработка на образците са използвани три подхода, както следва: само обезмасляване и промиване(без отстраняване на оксидния филм), механично полиране и комбинация между механично полиране с ецване в алкални разтвори. Параметрите на корозионния процес (поляризационно съпротивление, потенциал на питингообразуване и импедансен модул и капацитет) са използвани за количествено определяне на ефекта от предварителната подготовка. Установено е, че най-фективната предварителна повърхностна обработка по отношение на премахването на оксидния слой е механичното полиране. Проведените електрохимични изследвания доказаха, че подходът на ецване в алкални разтвори, използван най-често, съгласно голям брой статии, причинява образуването на филм, който не може да бъде премахнат, чрез просветляване в разредени разтвори на HNO_3. Процедурата на ецване би могла е подходяща за други алуминиеви сплави, но не е препоръчителна за сплавта АА2024.